

This discussion paper is/has been under review for the journal Earth System Dynamics (ESD). Please refer to the corresponding final paper in ESD if available.

# Early warning signals of tipping points in periodically forced systems

M. S. Williamson<sup>1</sup>, S. Bathiany<sup>2</sup>, and T. M. Lenton<sup>1</sup>

<sup>1</sup>Earth System Science group, College of Life and Environmental Sciences, University of Exeter, Laver Building, North Park Road, Exeter, EX4 4QE, UK

<sup>2</sup>Aquatic Ecology and Water Quality Management, Wageningen University, P.O. Box 47, Wageningen, the Netherlands

Received: 27 October 2015 – Accepted: 27 October 2015 – Published: 6 November 2015

Correspondence to: M. S. Williamson (m.s.williamson@exeter.ac.uk)

Published by Copernicus Publications on behalf of the European Geosciences Union.

ESDD

6, 2243–2272, 2015

Early warning signals

M. S. Williamson et al.

Title Page

Abstract

Introduction

Conclusions

References

Tables

Figures

◀

▶

◀

▶

Back

Close

Full Screen / Esc

Printer-friendly Version

Interactive Discussion



## Abstract

The prospect of finding generic early warning signals of an approaching tipping point in a complex system has generated much recent interest. Existing methods are predicated on a separation of timescales between the system studied and its forcing. However, many systems, including several candidate tipping elements in the climate system, are forced periodically at a timescale comparable to their internal dynamics. Here we find alternative early warning signals of tipping points due to local bifurcations in systems subjected to periodic forcing whose time scale is similar to the period of the forcing. These systems are not in, or close to, a fixed point. Instead their steady state is described by a periodic attractor. We show that the phase lag and amplification of the system response provide early warning signals, based on a linear dynamics approximation. Furthermore, the power spectrum of the system's time series reveals the generation of harmonics of the forcing period, the size of which are proportional to how nonlinear the system's response is becoming with nonlinear effects becoming more prominent closer to a bifurcation. We apply these indicators to a simple conceptual system and satellite observations of Arctic sea ice area, the latter conjectured to have a bifurcation type tipping point. We find no detectable signal of the Arctic sea ice approaching a local bifurcation.

## 1 Introduction

The potential for early warning of an approaching abrupt change or "tipping point" in a complex, dynamical system has been the focus of much recent research, see for example Scheffer et al. (2009), Lenton (2011) and Scheffer et al. (2012). Abrupt change in a system can occur due to a bifurcation – that is, a small smooth change in parameter values can result in a sudden or topological change in the system's attractors. Much work on the anticipation of bifurcations from time series data, e.g. in ecosystems (Scheffer et al., 2009), or the climate system (Dakos et al., 2008; Lenton, 2011),

# ESDD

6, 2243–2272, 2015

## Early warning signals

M. S. Williamson et al.

Title Page

Abstract

Introduction

Conclusions

References

Tables

Figures



Back

Close

Full Screen / Esc

Printer-friendly Version

Interactive Discussion



## Early warning signals

M. S. Williamson et al.

Title Page

Abstract

Introduction

Conclusions

References

Tables

Figures



Back

Close

Full Screen / Esc

Printer-friendly Version

Interactive Discussion



has been based on a clear separation of three time scales: (i) the time scale of the dynamics of the system one wants to study, (ii) much faster processes than the time scale of the system, and (iii) much slower processes than the time scale of the system. In addition, the system dynamics are modelled as overdamped, the fast dynamics as a noisy, normally distributed random variable of small variance and the slow dynamics as a constant, control parameter on the time scale of the system. Provided these are good working approximations, critical slowing down, the increase of the system's time scale, is expected prior to a local bifurcation and can be detected by computing the autocorrelation of a system's time series. An increasing trend in autocorrelation in time shows the stability of the system is weakening or equivalently, the system's time scale is increasing – which is a generic feature of a system approaching a local bifurcation. Provided the variance of the fast noisy process is constant, increasing variance of the system's time series is also a good indicator of critical slowing down, although it is less robust than autocorrelation due to its dependence on the noisy process.

For many systems of interest one or more of the above assumptions may be invalid. In particular, when the forcing of a system has a comparable period to the time scale of the system, the forcing cannot be modelled as a slow, constant control parameter or a fast, random process. Here we give alternative early warnings signals of approaching local bifurcations when the period of the forcing is similar to the time scale of the system. Systems of this type are particularly relevant in the climate system where periodic forcing is a consequence of the motion of the Earth relative to the Sun. For example, solar insolation variation from the diurnal, annual or Milankovich cycles. We look particularly at sinusoidal forcing since this approximates the variation of solar insolation well. However, the method works for any periodic forcing and we also give the derivation of the general case in the Appendix.

We show that increasing system time scale as it approaches a local bifurcation shows up as an increasing phase lag in the system response relative to the forcing. In addition, we show the amplitude of the system response increases as well. These indicators, like autocorrelation and variance in the usual method, assume the

## Early warning signals

M. S. Williamson et al.

Title Page

Abstract

Introduction

Conclusions

References

Tables

Figures



Back

Close

Full Screen / Esc

Printer-friendly Version

Interactive Discussion



linearized dynamics approximate the true nonlinear dynamics well. One might ask how well the linear approximation works, especially near the bifurcation, since bifurcations are strictly nonlinear phenomena. We show how to give a quantitative answer to this question by computing the power spectrum of the system's time series. In particular, as the system's behaviour becomes more nonlinear, harmonics of the forcing period are generated in the system response and their amplitudes may be obtained from the system's power spectra. Since the system response becomes more nonlinear as one approaches the bifurcation, one can view the increasing amplitude of harmonics as another early warning signal.

The paper is organised as follows: in Sect. 2 we introduce a conceptual model to illustrate periodically forced overdamped systems approaching a local bifurcation and the time scale separation problem. Then in Sect. 3 we show that the system response phase lag and amplification are good early warnings of approaching local bifurcations. These indicators, like previous ones, are based on a linear dynamics approximation, however in Sect. 4 we give another useful tool that allows one to quantify how good an approximation the linearized dynamics is as well as how nonlinear the system is behaving. In Sect. 5 we calculate these indicators for a conceptual model driven towards a local bifurcation and for satellite time series data of Arctic sea ice area, a system conjectured to be approaching a local bifurcation, before concluding in Sect. 6.

## 2 Periodically driven fold as an idealised example

Here we use an idealized example of a periodically forced, overdamped system tipping due to a local bifurcation to illustrate time scale separation between the forcing and the system's internal time scale. We first introduce our system which has one dynamical variable,  $x$ , (see Shneidman et al. (1994) and Jung and Hänggi (1993) for work on periodically driven, noisy double well systems).  $x$  evolves according to

$$\dot{x} = x - x^3 + D(t) \quad (1)$$

where overdots denote differentiation with respect to time,  $t$  and the periodic forcing function  $D(t)$  is

$$D(t) = D_m + D_a \cos(\omega t). \quad (2)$$

$D_m$  and  $D_a$  are constants and  $\omega = \frac{2\pi}{T}$  is the angular frequency and  $T$  is the period of the forcing. Equation (1) models a nonautonomous nonlinear system, the overdamped limit of a Duffing oscillator (Thompson and Stewart, 2002). When there is no periodic, just constant forcing ( $\omega = 0$ ) the familiar, well studied autonomous fold bifurcation is recovered (for example see Strogatz, 2001). For  $\omega = 0$ , the solutions of  $\dot{x} = 0$ , give the system's fixed points,  $x^*$  (the nullclines) and number either one or three depending on the value of  $D_m$ . One can evaluate the stability of these fixed points by looking at the linearized dynamics close to the fixed points,  $J(x^*)$

$$J(x^*) = \left. \frac{\partial \dot{x}}{\partial x} \right|_{x=x^*} = 1 - 3x^{*2}. \quad (3)$$

If  $J(x^*)$  is negative, the fixed point is stable, if it is positive it is unstable. In the region where three fixed points exist one finds two are stable and one is unstable. That is, it is a bistable region. The bistable region has boundaries marked by the local bifurcations and these can be found by solving  $J(x^*) = 0$  for  $x^*$  i.e. when the fixed point becomes neutrally stable. One can also calculate the  $e$  folding time scale of the system in state  $x$ ,  $\tau$  from the Jacobian  $\tau = -1/J(x)$ . We will refer to the  $e$  folding time as the system time scale. Early warning indicators are simply functions of  $J(x^*)$  or equivalently  $\tau$ .

## 2.1 Period of forcing much slower than system time scale, $\omega\tau \ll 1$

Now consider how the system can be described for the asymptotics of the forcing frequency  $\omega$ . First imagine that we force the system periodically, but very slowly. That is  $T \gg \tau$  and look at the behaviour of the system. Since  $D(t)$  is varying much slower than the system can respond, the system can adjust to the changing  $D(t)$  very quickly and

## Early warning signals

M. S. Williamson et al.

Title Page

Abstract

Introduction

Conclusions

References

Tables

Figures

◀

▶

◀

▶

Back

Close

Full Screen / Esc

Printer-friendly Version

Interactive Discussion







where

$$a = f(\bar{x}) - \frac{\partial f}{\partial x} \Big|_{x=\bar{x}} \bar{x} + D_m \quad (7)$$

$$\tau = -1 / \frac{\partial f}{\partial x} \Big|_{x=\bar{x}} \quad (8)$$

are the linearisation constants. We have assumed higher order terms such as  $\frac{1}{n!} \frac{\partial^n f}{\partial x^n} (x - \bar{x})^n$ ,  $n \geq 2$  are small relative to zeroth and first order terms so that the linearised dynamics approximates the full nonlinear dynamics well. We show how to check this approximation in Sect. 4. Assuming for the moment that this is a good approximation, one can solve Eq. (6) analytically. As  $t \gg \tau$  the system settles into the orbit

$$\lim_{t \gg \tau} x(t) = a\tau + \frac{D_a \tau}{\sqrt{1 + \omega^2 \tau^2}} \cos(\omega t + \phi) \quad (9)$$

where the system response lags the forcing by phase  $\phi_{\text{lag}} = \omega t_{\text{lag}} = -\phi$  given by

$$\phi_{\text{lag}} = \arctan(\omega\tau) \quad (10)$$

that is, the phase lag is a function of the forcing frequency and the system response time scale. One also notices that the system response, relative to the forcing amplitude,  $D_a$ , is amplified by a factor

$$\frac{\tau}{\sqrt{1 + \omega^2 \tau^2}} \quad (11)$$

which is also a direct function of  $\omega$  and  $\tau$ . We save the more general derivation when  $D(t)$  can be any periodic function to Appendix .

## Early warning signals

M. S. Williamson et al.

Title Page

Abstract

Introduction

Conclusions

References

Tables

Figures

◀

▶

◀

▶

Back

Close

Full Screen / Esc

Printer-friendly Version

Interactive Discussion



## 3.1 Asymptotics of the early warning indicators and examples of systems in these limits

### 3.1.1 $\omega\tau \gg 1$ , Terrestrial carbon cycle forced by annual solar insolation

Consider the asymptotics of Eq. (10). When the system is losing stability and approaching a local bifurcation its time scale becomes very large,  $\tau \gg T$ , and the system phase lag becomes  $\phi_{\text{lag}} \rightarrow \pi/2$ . That is, the system response lags the forcing by quarter of a cycle. This limit is also appropriate for systems where the periodic forcing is much quicker than the time scale of the system. Unfortunately, inferring a time scale of a system with  $\phi_{\text{lag}} \rightarrow \pi/2$  is not possible to do reliably from the phase lag as  $\phi_{\text{lag}}$  asymptotes to this value. One can only reliably conclude  $\tau \gg T$ .

The system response amplification in the  $\tau \gg T$  limit  $\rightarrow \frac{1}{\omega}$ . That is, system response amplitude is related to the forcing amplitude,  $D_a$ , by  $\frac{D_a}{\omega}$ .

An example of a system approximately modelled by this limit is the global terrestrial vegetation carbon which has a dominant timescale on the order of decades, much larger than its periodic forcing, the annual cycle of solar insolation. This dominant time scale comes from the large long term carbon storage e.g. the time scale taken for a forest to regrow once cut down. One sees this phase lag of quarter of a cycle in the annual minimum of the Mauna Loa  $\text{CO}_2$  record<sup>1</sup> relative to the Northern Hemisphere solar insolation maximum. This lagged annual minimum in the integrated response of the total atmospheric carbon results from the dominance of the Northern Hemisphere's mid latitude terrestrial vegetation carbon in the global carbon flux. We have plotted the Mauna Loa  $\text{CO}_2$  record and the time of year of the minimum concentration in Fig. 2.

<sup>1</sup>Dr. Pieter Tans, NOAA/ESRL ([www.esrl.noaa.gov/gmd/ccgg/trends/](http://www.esrl.noaa.gov/gmd/ccgg/trends/)) and Dr. Ralph Keeling, Scripps Institution of Oceanography ([scrippsco2.ucsd.edu/](http://scrippsco2.ucsd.edu/)).

Title Page

Abstract

Introduction

Conclusions

References

Tables

Figures

◀

▶

◀

▶

Back

Close

Full Screen / Esc

Printer-friendly Version

Interactive Discussion



### 3.1.2 $\omega\tau \ll 1$ , Ice sheet dynamics forced by Milankovitch cycles

When  $T \gg \tau$ , there is no phase lag,  $\phi_{\text{lag}} \rightarrow 0$ , and the system can respond instantly.

The system response amplitude in this limit  $\rightarrow \tau$ . That is, system response amplitude is related to the forcing amplitude,  $D_a$ , by  $D_a\tau$ .

5 An example of a system that has the correct time scale separation and periodic forcing are the glacial/interglacial cycles that have the slow build, fast collapse type behaviour of relaxation oscillations. Ice sheets have time scales in the order of thousands of years forced by the solar insolation variation of Milankovitch cycles. The forcing is a superposition of many different sinusoidal frequencies, the dominant ones having  
10 periods of 41 kyr (related to the obliquity of Earth's orbit), 19 and 23 kyr (related to the precession). Current thinking however, favours more complex, two and higher dimensional dynamics to model these cycles than the single variable models we consider in this paper (Saltzman, 2002; Crucifix, 2012, 2013; Saedeleer et al., 2013).

### 3.1.3 $\omega\tau \sim 1$ , Ocean mixed layer temperature forced by annual solar insolation

15 The intermediate regime, when  $\tau \sim T$  (the time scale of the system is approximately the same as the forcing period) is where phase lag and response amplification are most useful as early warning indicators as one sees values somewhere between the two limits.

To give an example of a system operating in this regime consider the annual variation in sea temperatures in Northern Hemisphere temperate regions. A rough estimate of the ocean surface mixed layer time scale gives  $\tau \sim 10$  months and this surface layer is heated by the annual cycle of solar insolation to varying degrees throughout the year. Calculation of the phase lag for this  $\tau$  and  $T$  yields a lag of about 2.6 months i.e. roughly the maximal and minimal sea temperatures are in September and March. Arctic sea  
20 ice extent also falls into this regime and will be one of the systems we apply the early warning indicators to in Sect. 5.2.

## 4 System nonlinearity from Fourier analysis

By simply looking at the time series of the system response and the forcing one can determine what the amplitude and phase lag are when the driving is of the form Eq. (2) and the system response is approximately linear. However, the system is essentially nonlinear and these nonlinear effects may become large near a bifurcation or when the system is driven hard. By taking the Fourier transform of the time series of the system response one can quantify how large these nonlinear effects are.

Once the system has settled into an orbit of period  $T$ , we can write the full nonlinear response of an arbitrary system as a Fourier series, a sum of  $N$  sinusoidal functions with angular frequencies  $\omega_n = \frac{2\pi n}{T}$ , amplitudes  $A_n$  and phases  $\phi_n$  i.e.

$$x(t) = \sum_{n=0}^N A_n \cos(\omega_n t + \phi_n). \quad (12)$$

The  $n = 0$  component is a constant, the long term mean of the response, the  $n = 1$  component is the linear response of the system and the  $n \geq 2$  components are the  $n$ th order harmonics and come about from the nonlinear response of the system. Since the system has settled into a periodic orbit the system must repeat itself every cycle. The only way the system can do this is by adding harmonics to linear response. By looking at the ratios  $\frac{A_n}{A_1}$  for  $n \geq 2$  we can see how important the nonlinear effects are relative to the linear approximation. In practice the largest harmonics will generally be the 2nd ( $n = 2$ ) and 3rd order ( $n = 3$ ) harmonics and provided they are an order of magnitude (10 times,  $\frac{A_n}{A_1} < 10^{-1}$ ) less than the fundamental harmonic, the linear analysis in the last section works well.

One may also expect subharmonics, components that have periods that are integer multiples of the forcing period, to be observed in the system response. Subharmonics

Title Page

Abstract

Introduction

Conclusions

References

Tables

Figures



Back

Close

Full Screen / Esc

Printer-friendly Version

Interactive Discussion



are not possible in the systems we consider here due to the dimensionality of the phase space.<sup>2</sup>

Calculation of the amplitudes,  $A_n$ , is via a Fourier transform of the time series. To do this, we choose to represent the system response, Eq. (12), in the more convenient but equivalent form

$$x(t) = \sum_{n=-N}^N c_n e^{i\omega_n t} \quad (13)$$

where we have defined  $c_n = \frac{A_n}{2} e^{i\phi_n}$  and  $c_{-n} = c_n^*$ . We then take the Fourier transform of this form to find the  $c_n$

$$c_n = \frac{1}{T} \int_0^T x(t) e^{-i\omega_n t} dt \quad (14)$$

so the amplitude  $A_n$  associated to the  $n$ th harmonic is given by

$$A_n = 2|c_n|. \quad (15)$$

One can also find the phases,  $\phi_n$  by taking the argument of  $c_n$ .

<sup>2</sup>Systems described by Eq. (4) are completely described by the two dimensional space of variables  $x$  and  $t$ . Recasting the nonautonomous system in Eq. (4) as a two dimensional autonomous system by identifying a new angular variable  $\phi = \omega t$ , the system is then described by  $\dot{x} = f(x) + D(\phi)$  and  $\dot{\phi} = \omega$ . The resulting phase space  $(x, \phi)$  is then cylindrical as  $\phi$  is  $2\pi$  modular. If subharmonics are possible in the periodic system response the trajectory must wind around the cylinder at least twice before repeating itself. Such a trajectory implies it crosses itself which is not allowed due to the existence and uniqueness theorem. Therefore subharmonics cannot exist in the two dimensional systems. This is of course not true for three and higher dimensional systems.

**Early warning signals**

M. S. Williamson et al.

Title Page	
Abstract	Introduction
Conclusions	References
Tables	Figures
◀	▶
◀	▶
Back	Close
Full Screen / Esc	
Printer-friendly Version	
Interactive Discussion	



## Early warning signals

M. S. Williamson et al.

Title Page

Abstract

Introduction

Conclusions

References

Tables

Figures

◀

▶

◀

▶

Back

Close

Full Screen / Esc

Printer-friendly Version

Interactive Discussion



Since the ratios  $\frac{A_n}{A_1} \equiv \frac{|c_n|}{|c_1|}$  measure how nonlinear the system is one expects these to increase as the system approaches a bifurcation as well as quantitative measures of how appropriate the linear analysis is. We demonstrate the linear early warning indicators and the Fourier analysis in the next section.

## 5 Examples

### 5.1 Conceptual model

We now demonstrate how one might use these indicators to detect changing system time scale (equivalently changing system stability) and therefore the anticipation of an approaching local bifurcation. We demonstrate this with the conceptual system in Eq. (1). We assume the forcing amplitude  $D_a$  and the period  $T \sim O(\tau)$  are fixed and  $D_m$  is a control parameter, slowly varying from negative values towards the local bifurcation. We expect to see the system response become more phase lagged and amplified as we approach the local bifurcation at  $D_m \approx 0.33$  when approaching from the lower nullcline solutions.

In our example we choose to tip the system from one state to another by slowly altering the mean of the driving  $D_m$ . We could, however, have tipped the system by changing one of the other driving parameters such as amplitude  $D_a$  or frequency  $\omega$ . Since the system response amplitude depends on  $D_a$  and  $\omega$  and phase lag depends on  $\omega$ , one must take this into account when inferring system time scales from the indicators.

In Fig. 3 we run the system forward in time, linearly varying  $D_m$  from  $-2$  to  $2$  across the bifurcation over about 25 cycles of the forcing period (for the values of the parameters see the figure caption). In Fig. 4 we have plotted the phase lag and amplitude of the system response prior to the bifurcation at around  $t/T = 15$  which are both increasing as the bifurcation is approached due to the increase in  $\tau$ . Phase lag is calculated from the difference between the times of the maxima in the forcing and the system response

## Early warning signals

M. S. Williamson et al.

Title Page

Abstract

Introduction

Conclusions

References

Tables

Figures



Back

Close

Full Screen / Esc

Printer-friendly Version

Interactive Discussion



in each cycle. Response amplitude is calculated by taking half the difference between the maximal and minimal values in the system response in each cycle.

We also plot the ratios  $A_n/A_1$  against  $T_n/T$  derived from a Fourier transform of the system response in Fig. 5. In the upper panel all parameters are the same as Fig. 3 except we have fixed  $D_m$  in each of the two runs. In the first run  $D_m = -2$ , this is far from the bifurcation and one expects the system to behave more linearly (blue line). One sees a second harmonic around 2 orders of magnitude smaller than the linear response. In the second run  $D_m = 0.25$  and the orbit is much closer to the bifurcation (red line). The second harmonic has increased to about an order of magnitude smaller than the fundamental harmonic and a third harmonic is now also visible indicating the system has become more nonlinear.

We illustrate the spectrum of very nonlinear dynamics in the lower panel of Fig. 5. This is the spectrum of the slow forcing run with the same parameters in Fig. 1 (red line) that had a response that resembled relaxation oscillations. For these parameters the dynamics is very nonlinear as shown by the large amplitude of the harmonics. Notice only odd harmonics appear in its spectrum. This is because the static potential  $V = -\int \dot{x} dx$  is symmetric about  $x$  for this value of  $D_m = 0$  i.e.  $V(x) = V(-x)$  and therefore any solution of  $\dot{x}$  must also have this symmetry,  $x(t+T/2) = -x(t)$ . Only odd harmonics have this property.<sup>3</sup>

<sup>3</sup>This is not sufficient though as there are other parameter settings that feature the second harmonic and also have the same symmetric potential i.e.  $D_m = 0$  and  $T = \pi$  in Fig. 1 (blue line). The difference is that the runs featuring second harmonic responses only experience a limited part of the potential, not the full symmetric potential. Even though the potential is the same, the forcing is quick enough to trap the system in an orbit in just one of the two potential wells. This local potential well is asymmetric and what the system sees is effectively described by a Taylor expansion around the centre of that well. In contrast the relaxation oscillation type run travels across both wells equally and therefore sees the global symmetric potential requiring an odd harmonic solution. This is not a generic case however.

## 5.2 Arctic sea ice satellite observations

There has been much research in to a possible local bifurcation and tipping point in the Arctic sea ice without a clear consensus emerging, see for example Armour et al. (2011), Eisenman and Wettlaufer (2009), Lindsay and Zhang (2005), Livina and Lenton (2013), Ridley et al. (2012) and Wang and Overland (2012). This possible bifurcation in the sea ice cover may be due to the well known ice albedo feedback first studied by Budyko (1969) and Sellers (1969). When ice is present it reflects a high proportion of the incoming solar radiation due to its higher albedo yet when it starts receding the darker ocean absorbs more radiation increasing heating and promoting more sea ice retreat. This feedback can result in instability and multiple steady states.

We analyze a time series of Arctic sea ice area satellite observations from 1979 to present data and calculate the phase lag, response amplitude and spectrum of the time series to look for signs of critical slowing down. In Fig. 6 we have plotted the Arctic sea ice area against year. Sea ice area data were obtained from The Cryosphere Today project of the University of Illinois. This dataset<sup>4</sup> uses SSM/I and SMMR series satellite products and spans 1979 to present at daily resolution.

In Fig. 7 we plot the amplitude of the sea ice area annual cycle and the phase lag between the sea ice area minimum and maximum during each cycle. We assume the maximal and minimal driving occurs at the same time as maximal and minimal of the solar insolation, that is, the midpoint and end point of the year respectively to obtain phase lags. To limit the the impact of high frequency variability on the location of the extrema, we have smoothed the daily data with a sliding window with 30 days.

From Fig. 7 we see the cycle amplitude is increasing with time although the phase lag does not appreciably change. We first make some rough calculations to see if these plots are consistent with each other: from the phase lag figure, a time scale of  $\tau \sim [0.33, 0.5]$  yr from the lag of  $[0.18, 0.2]$  of a cycle can be inferred. If we assume for the moment, the amplitude of the forcing  $D_a$  is not changing throughout the time

<sup>4</sup><http://arctic.atmos.uiuc.edu/cryosphere/timeseries.anom.1979-2008>

Title Page

Abstract

Introduction

Conclusions

References

Tables

Figures



Back

Close

Full Screen / Esc

Printer-friendly Version

Interactive Discussion



## Early warning signals

M. S. Williamson et al.

Title Page

Abstract

Introduction

Conclusions

References

Tables

Figures



Back

Close

Full Screen / Esc

Printer-friendly Version

Interactive Discussion



period of the observations (this may not be true) and take the smallest value in the range for  $\tau_{1978} = 0.33$  yr at occurring in 1978 and the largest value in 2015,  $\tau_{2015} = 0.5$  yr we can make a rough calculation of how much the sea ice amplitude would have

increased i.e.  $\frac{A_{2015}}{A_{1978}} = \frac{\tau_{2015}}{\tau_{1978}} \sqrt{\frac{1 + \omega^2 \tau_{1978}^2}{1 + \omega^2 \tau_{2015}^2}} \approx 1.06$ . From Fig. 7 we take the amplitude at 1978

to be  $A_{1978} \sim 4.5$  and at 2015 to be  $A_{2015} \sim 5$  we find  $\frac{A_{2015}}{A_{1978}} = 1.11$ . These values could therefore be consistent with a constant  $D_a$  and a changing time scale. However, the time scales inferred from either the phase lag or amplitude are not changing appreciably and therefore it seems unlikely the system is approaching a local bifurcation.

We note that the phase lag is a more robust indicator. This is because the phase lag depends only on the product of the frequency of the forcing and the system time scale whereas the amplitude depends additionally on the amplitude of the driving,  $D_a$ , which may well be changing throughout the observational period and could account for some or all of the increase seen in the amplitude in Fig. 7. Although the solar insolation will be a large component of the forcing amplitude and is essentially fixed, other factors such as clouds as well as air and sea temperatures will also factor into the driving amplitude. Geometrical constraints imposed by land masses affecting the maximal extent of the sea ice will also influence the amplitude of the sea ice oscillation when ice extent is large (Eisenman, 2010). In contrast, we can take the frequency of the driving to be essentially fixed by the annual solar insolation cycle making the phase lag more robust.

We have also plotted the ratios  $A_n/A_1$  for the entire time series in Fig. 8. We note the nonlinear effects are quite prominent in this system, second and third harmonics are around an order of magnitude smaller than the linear response, although we can still probably get away with the linear analysis. These nonlinearities may be due to albedo effect or to the geometrical effects of the Arctic ocean basin (Eisenman, 2010).

To conclude, from this simple analysis it seems that the system's time scale and therefore stability is not changing appreciably if at all and it is unlikely to be approaching a local bifurcation. However, simple theoretical models, such as Eisenman and Wett-

laufer (2009) and Eisenman (2012) suggest that the sea ice time scale does not change very much approaching the bifurcation, even decreasing slightly before rapidly changing over a very small interval and therefore would be very hard to detect if present.

## 6 Conclusions

5 Much previous work on detecting local bifurcations from time series required one to be able to partition the universe into widely separated time scales and model the system dynamics as overdamped. When this is the case one can use the usual early warning indicators of increasing autocorrelation and variance since these indicators measure the system's response to small perturbations away from its fixed point by the fast, noisy processes. It is the response to this small, noisy forcing that allows one to measure the system's time scale. The systems we have been looking at in this paper do not have fast or random forcing. The systems considered here have deterministic forcing with a period roughly that of its time scale although the dynamics are still overdamped. Deterministic forcing again allows one to infer the system's time scale simply by measuring the response to the forcing. We found two analogous early warning indicators to the autocorrelation and variance in these systems; these were phase lag and response amplification respectively. Just as autocorrelation is more robust as an indicator (it is a function of fewer parameters), the same is true of phase lag, only depending on the frequency of the forcing and the time scale of the system. The system response amplification also depends on the amplitude of forcing, which in many circumstances is probably difficult to measure.

We also showed that by taking a Fourier transform of the time series one can quantify how nonlinear the system is behaving and whether the linear approximations usually made are good.

25 We applied these new indicators to satellite observations of Arctic sea ice area, a system whose period of forcing, effectively the annual cycle of insolation, is similar to the time scale of the system. This is also a system that has been conjectured to have

## Early warning signals

M. S. Williamson et al.

Title Page

Abstract

Introduction

Conclusions

References

Tables

Figures



Back

Close

Full Screen / Esc

Printer-friendly Version

Interactive Discussion



a tipping point due to a local bifurcation. We did not find any detectable critical slowing down and therefore signs of this bifurcation. It should be noted however simple models of the sea ice suggest critical slowing down only occurs very close to the bifurcation making it very hard to detect.

## 5 Appendix: Early warnings with arbitrary periodic forcing

Here we give the derivation for the more general case of any type of periodic forcing  $D$ . That is we solve the equation

$$\dot{x} + \frac{x}{\tau} = D(t). \quad (\text{A1})$$

10  $\tau$  the timescale of the system (the  $e$  folding time). For any periodic forcing,  $D(t)$  with period  $T$  can be written as the Fourier series

$$D(t) = \sum_{i=0}^N B_i \cos(\omega_i t + \chi_i). \quad (\text{A2})$$

15  $B_i$  are the amplitudes of the different component sinusoidal waves,  $\omega_i = \frac{2\pi i}{T}$  are the frequencies of the components and  $\chi_i$  are the phases of each of the components. As the equation is linear the superposition principle holds. That is, we assume the solution has the form

$$x(t) = \sum_{i=0}^N x_i(t) \quad (\text{A3})$$

by setting all but the  $i$ th term of the driving to zero we can solve the  $N + 1$  equations

$$\dot{x}_i + \frac{x_i}{\tau} = B_i \cos(\omega_i t + \chi_i) \quad (\text{A4})$$

Title Page

Abstract

Introduction

Conclusions

References

Tables

Figures

◀

▶

◀

▶

Back

Close

Full Screen / Esc

Printer-friendly Version

Interactive Discussion



for each  $x_i(t)$  which is just the same as the original sinusoidally forced equation. We can then superpose them to obtain the full solution to any periodic driving term. The solution of the forced system is

$$x(t) = \sum_{i=0}^N \frac{\tau B_i}{\sqrt{1 + \omega_i^2 \tau^2}} [\cos(\omega_i t + \chi_i - \arctan(\omega_i \tau)) - e^{-\frac{t}{\tau}} \cos(\chi_i - \arctan(\omega_i \tau))] + x_0 e^{-\frac{t}{\tau}} \quad (\text{A5})$$

which settles into orbit

$$x(t) = \sum_{i=0}^N \frac{\tau B_i}{\sqrt{1 + \omega_i^2 \tau^2}} \cos(\omega_i t + \chi_i - \arctan(\omega_i \tau)) \quad (\text{A6})$$

when  $t \gg \tau$ , that is, the solution is just the sum of each of the forcing components  $i$ , each with a response amplification of

$$\frac{\tau}{\sqrt{1 + \omega_i^2 \tau^2}} \quad (\text{A7})$$

and a response lagging the forcing with a phase of

$$\phi_i^{\text{lag}} = \arctan(\omega_i \tau). \quad (\text{A8})$$

One can find out what these phase lags and amplitudes are by taking the Fourier transform of the time series of both the forcing and response.

15 *Acknowledgements.* The research leading to these results has received funding from the European Union Seventh Framework Programme FP7/2007-2013 under grant agreement no. 603864 (HELIX). We are also grateful to Peter Ashwin, Peter Cox, Michel Crucifix, Vasilis Dakos, Henk Dijkstra, Jan Sieber, Marten Scheffer and Appy Sluijs for the fruitful discussions over beers and balls.

Title Page

Abstract

Introduction

Conclusions

References

Tables

Figures

◀

▶

◀

▶

Back

Close

Full Screen / Esc

Printer-friendly Version

Interactive Discussion



## References

- Armour, K. C., Eisenman, I., Blanchard-Wrigglesworth, E., McCusker, K. E., and Bitz, C. M.: The reversibility of sea ice loss in a state-of-the-art climate model, *Geophys. Res. Lett.*, 38, L16705, doi:10.1029/2011GL048739 2011. 2257
- 5 Budyko, M. I.: The effect of solar radiation variations on the climate of the Earth, *Tellus*, 21, 611–619, 1969. 2257
- Crucifix, M.: Oscillators and relaxation phenomena in Pleistocene climate theory, *Philos. T. Roy. Soc. A*, 370, 1140–1165, 2012. 2252
- Crucifix, M.: Why could ice ages be unpredictable?, *Clim. Past*, 9, 2253–2267, doi:10.5194/cp-9-2253-2013, 2013. 2252
- 10 Dakos, V., Scheffer, M., van Nes, E. H., Brovkin, V., Petoukhov, V., and Held, H.: Slowing down as an early warning signal for abrupt climate change, *P. Natl. Acad. Sci. USA*, 105, 14308–14312, 2008. 2244
- Eisenman, I.: Geographic muting of changes in the Arctic sea ice cover, *Geophys. Res. Lett.*, 37, L16501, doi:10.1029/2010GL043741, 2010. 2258
- 15 Eisenman, I.: Factors controlling the bifurcation structure of sea ice retreat, *J. Geophys. Res.*, 117, D01111, doi:10.1029/2011JD016164, 2012. 2259
- Eisenman, I. and Wettlaufer, J. S.: Nonlinear threshold behaviour during the loss of Arctic sea ice, *P. Natl. Acad. Sci. USA*, 106, 28–32, 2009. 2257, 2258
- 20 Jung, P., and Hänggi, P.: Hopping and phase shifts in noisy periodically driven bistable systems, *Z. Phys. B Con. Mat.*, 90, 255–260, 1993. 2246
- Lenton, T. M.: Early warning of climate tipping points, *Nat. Clim. Change*, 1, 201–209, 2011. 2244
- Lindsay, R. W. and Zhang, J.: The thinning of the Arctic sea ice, 1988–2003: Have we passed a tipping point?, *J. Climate*, 18, 4879–4894, 2005. 2257
- 25 Livina, V. N. and Lenton, T. M.: A recent tipping point in the Arctic sea-ice cover: abrupt and persistent increase in the seasonal cycle since 2007, *The Cryosphere*, 7, 275–286, doi:10.5194/tc-7-275-2013, 2013. 2257
- Ridley, J. K., Lowe, J. A., and Hewitt, H. T.: How reversible is sea ice loss?, *The Cryosphere*, 6, 193–198, doi:10.5194/tc-6-193-2012, 2012. 2257
- 30

## ESDD

6, 2243–2272, 2015

### Early warning signals

M. S. Williamson et al.

Title Page

Abstract

Introduction

Conclusions

References

Tables

Figures

◀

▶

◀

▶

Back

Close

Full Screen / Esc

Printer-friendly Version

Interactive Discussion



## Early warning signals

M. S. Williamson et al.

Title Page

Abstract

Introduction

Conclusions

References

Tables

Figures

◀

▶

◀

▶

Back

Close

Full Screen / Esc

Printer-friendly Version

Interactive Discussion



Saedeleer, B. D., Crucifix, M., and Wieczorek, S.: Is the astronomical forcing a reliable and unique pacemaker for climate? A conceptual model study, *Clim. Dynam.*, 40, 273–294, 2013. 2252

Saltzman, B.: *Dynamical Paleoclimatology: Generalized Theory of Global Climate Change*, Academic Press, 2002. 2252

Scheffer, M., Bacompte, J., Brock, W. A., Brovkin, V., Carpenter, S. R., Dakos, V., Held, H., van Nes, E. H., Rietkerk, M., and Sugihara, G.: Early warning signals for critical transitions, *Nature*, 461, 53–59, 2009. 2244

Scheffer, M., Carpenter, S. R., Lenton, T. M., Bascompte, J., Brock, W., Dakos, V., van de Koppel, J., van de Leemput, I. A., Levin, S. A., van Nes, E. H., Pascual, M., and Vandermeer, J.: Anticipating critical transitions, *Science*, 338, 344–348, 2012. 2244

Sellers, W. D.: A global climate model based on the energy balance of the Earth-atmosphere system, *J. Appl. Meteorol.*, 8, 392–400, 1969. 2257

Shneidman, V. A., Jung, P., and Hänggi, P.: Power spectrum of a driven bistable system, *Europhys. Lett.*, 26, 571–576, 1994. 2246

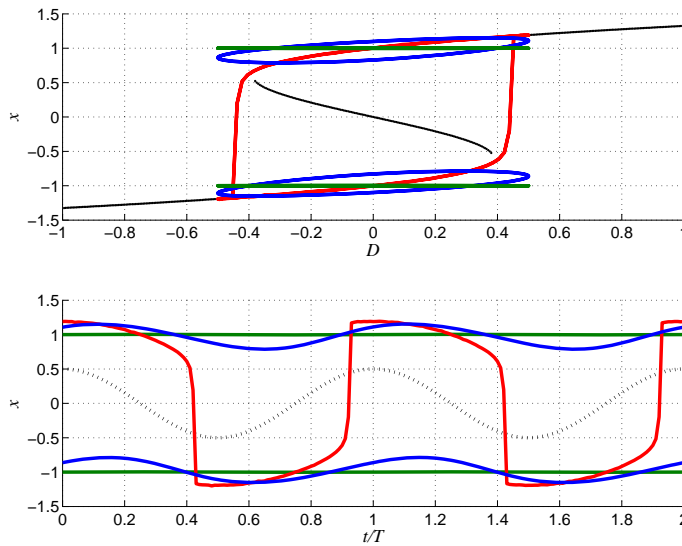
Strogatz, S. H.: *Nonlinear Dynamics and Chaos*, Westview Press, 2001. 2247

Thompson, J. M. T. and Stewart, H. B.: *Nonlinear Dynamics and Chaos*, 2nd Edn., John Wiley and Sons, Ltd., 2002. 2247

Wang, M. and Overland, J. E.: A sea ice free summer Arctic within 30 years: an update from CMIP5 models, *Geophys. Res. Lett.*, 39, L18501, doi:10.1029/2012GL052868, 2012. 2257

## Early warning signals

M. S. Williamson et al.



Title Page

Abstract

Introduction

Conclusions

References

Tables

Figures



Back

Close

Full Screen / Esc

Printer-friendly Version

Interactive Discussion



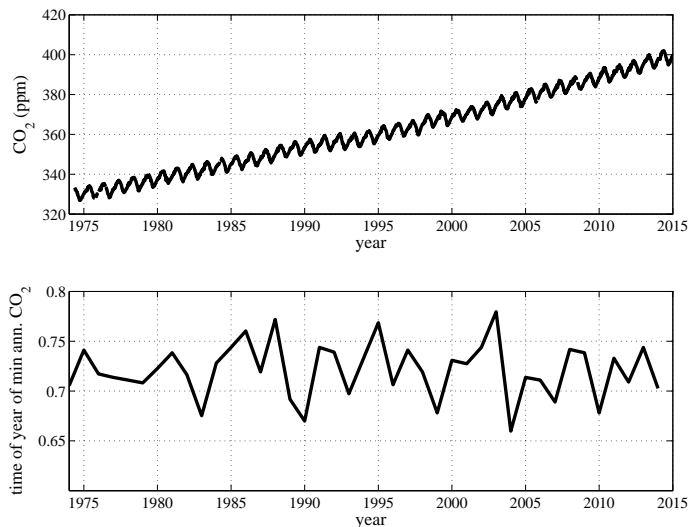
**Figure 1.** The dynamics of the system described by Eq. (1) in three different time scale regimes. Forcing parameters are set to  $D_m = 0$ ,  $D_a = 1/2$ . In the upper panel system state  $x$  is plotted against  $D(t)$ . The black lines are the nullclines and the coloured lines are the system responses for different periods of forcing. In the lower panel  $x$  is plotted against the number of cycles,  $t/T$ , once the system has reached a steady state. The dotted line is the forcing,  $D(t)$  while the colored lines are the system responses. The red line is for the slow forcing limit,  $\tau \ll T$ ,  $T = 100\pi$  so  $\omega\tau \approx 1/100$ . As the system time scale is much faster than the change in the forcing, the system essentially “sticks” to the fixed points until they become unstable at the bifurcations and jump to a different attractor. One can regard the system response in two different ways: (i) a single periodic attractor giving a relaxation oscillations in a monostable region. (ii) Tipping between point attractors by crossing local bifurcations in a bistable region. This tipping causes the dynamics to be very nonlinear. The green line is the fast forcing limit,  $T \ll \tau$ ,  $T = \pi/100$  so  $\omega\tau \approx 100$ . There are two possible stable attractors for this set of values. As the system time scale is much slower than the change in the forcing, the system essentially remains static and all the dynamics come from the forcing itself. Although it is hard to see in the figure due to the small amplitude system response, the lag relative to the forcing is  $1/4$  of a cycle and the dynamics are approximately linear. The blue line is the intermediate regime,  $\tau \sim T$ ,  $T = \pi$  so  $\omega\tau \approx 1$  and there are two possible stable attractors for this set of values. As the system time scale is approximately the same as the period of the forcing, the system response is a competition between the system’s tendency to decay towards the nullcline and the forcing pushing it away setting up a stable orbit. Notice there is some phase lag and the dynamics look approximately linear.

## Early warning signals

M. S. Williamson et al.

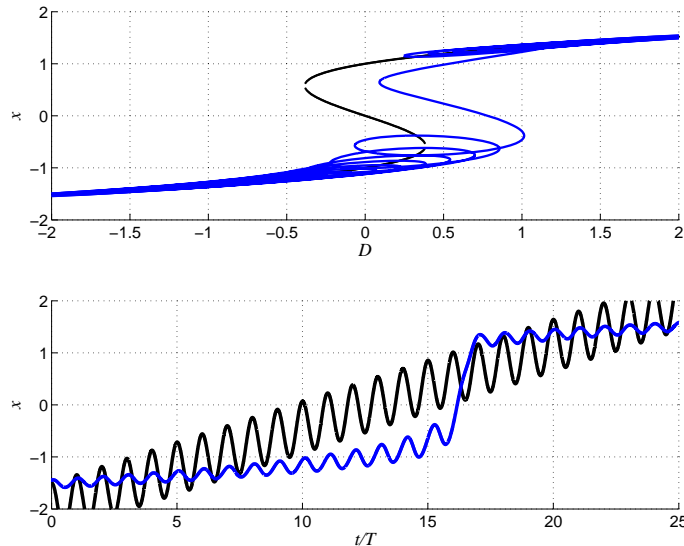
Title Page	
Abstract	Introduction
Conclusions	References
Tables	Figures
◀	▶
◀	▶
Back	Close
Full Screen / Esc	
Printer-friendly Version	
Interactive Discussion	





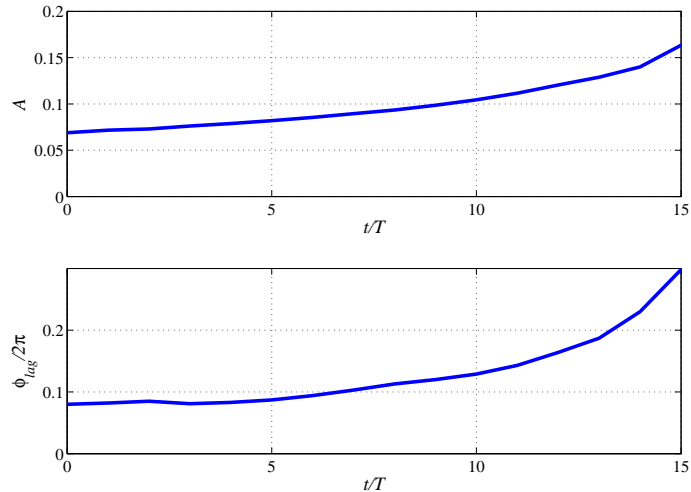
**Figure 2.** Atmospheric CO<sub>2</sub> concentration recorded at Mauna Loa against time in the upper panel. In the lower panel we have plotted the minimum annual CO<sub>2</sub> concentration against year. One notices the minimum CO<sub>2</sub> concentration occurs roughly 3/4 of the way through the year. This is because maximal carbon uptake occurs during the Northern Hemisphere summer from the terrestrial vegetation and it is maximally lagged behind the maximum in the Northern Hemisphere solar insolation (best growing conditions) by 1/4 of a cycle because of the time scale difference between the response of the system and the period of the forcing. In this case the system is the terrestrial vegetation which has a timescale of decades and the periodic forcing is the annual cycle of solar insolation.

[Title Page](#)[Abstract](#)[Introduction](#)[Conclusions](#)[References](#)[Tables](#)[Figures](#)[Back](#)[Close](#)[Full Screen / Esc](#)[Printer-friendly Version](#)[Interactive Discussion](#)



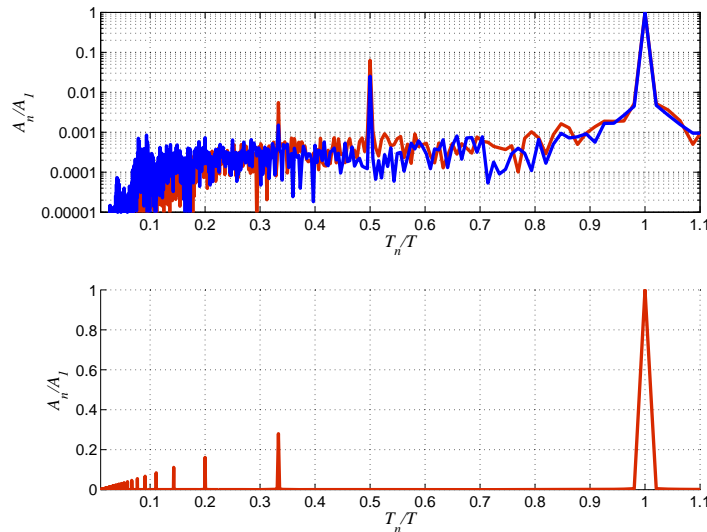
**Figure 3.** The dynamics of the system are described by Eq. (1) with varying  $D_m$ . Parameters are set to  $D_a = 1/2$ ,  $T = \pi$  (the same order as the system time scale  $\tau$ ) and  $D_m$  is varied linearly with time between  $-2$  and  $2$  over about 25 cycles. In the upper panel the black lines are the nullclines while the system response is the blue line plotted against  $D(t)$ . The orbit loses stability around a mean value of  $D \approx 0.5$  and jumps to a new orbit. In the lower panel we have plotted the system response (blue) against the forcing  $D$  against  $t/T$ . One can see the loss of stability of the orbit around  $t/T \approx 15$  and the prior increase in system response amplitude.

[Title Page](#)
[Abstract](#)
[Introduction](#)
[Conclusions](#)
[References](#)
[Tables](#)
[Figures](#)
[◀](#)
[▶](#)
[◀](#)
[▶](#)
[Back](#)
[Close](#)
[Full Screen / Esc](#)
[Printer-friendly Version](#)
[Interactive Discussion](#)

**Figure 4.** The early warning indicators, response amplification (upper panel),  $A = \frac{D_a \tau}{\sqrt{1 + \omega^2 \tau^2}}$ , and phase lag (lower panel),  $\frac{\phi_{lag}}{2\pi} = \frac{1}{2\pi} \arctan(\omega\tau)$  calculated for the time series in Fig. 3. We have plotted these indicators prior to the bifurcation at  $t/T \approx 15$ . Note both indicators are increasing as one would expect.

[Title Page](#)
[Abstract](#)
[Introduction](#)
[Conclusions](#)
[References](#)
[Tables](#)
[Figures](#)
[◀](#)
[▶](#)
[◀](#)
[▶](#)
[Back](#)
[Close](#)
[Full Screen / Esc](#)
[Printer-friendly Version](#)
[Interactive Discussion](#)




**Figure 5.** Ratio of the  $n$ th order harmonic amplitude to the fundamental harmonic amplitude  $A_n/A_1$  against the ratio of the  $n$ th harmonic period to the fundamental harmonic period  $T_n/T$ . The dynamics of the system are described by Eq. (1). Parameters are fixed to  $D_a = 1/2$ ,  $T = \pi$  (the same order as the system time scale  $\tau$ ) for the upper panel. The blue line is for  $D_m = -2$  (far away from the bifurcation), the nonlinear response is dominated by the second harmonic at  $T_n/T = 1/2$  although small, about two orders of magnitude less than the linear response. The red line is  $D_m = 1/4$ , close to the bifurcation the system response has become more nonlinear. The second harmonic ( $T_n/T = 1/2$ ) is now almost one order of magnitude less and the third order harmonic ( $T_n/T = 1/3$ ) is also prominent. In the bottom panel, we show the spectrum when the dynamics is very nonlinear. Parameters are set to  $D_m = 0$ ,  $D_a = 1/2$ ,  $T = 100\pi$  so  $\omega\tau \approx 1/100$ . This is the slow forcing limit shown in Fig. 1 (red line) which has a very nonlinear relaxation oscillation type response. Note only odd harmonics ( $T_n/T = 1/3, 1/5, 1/7, \dots$  etc.) are present due to the system experiencing a symmetric potential requiring the solution,  $x(t)$ , to also have this symmetry.

[Title Page](#)
[Abstract](#)
[Introduction](#)
[Conclusions](#)
[References](#)
[Tables](#)
[Figures](#)
[◀](#)
[▶](#)
[◀](#)
[▶](#)
[Back](#)
[Close](#)
[Full Screen / Esc](#)
[Printer-friendly Version](#)
[Interactive Discussion](#)


## Early warning signals

M. S. Williamson et al.

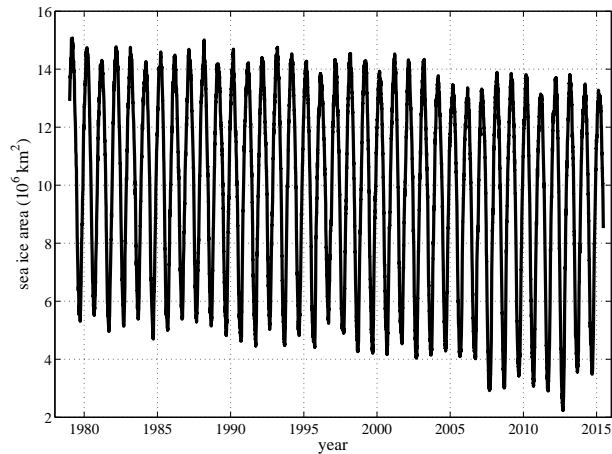


**Figure 6.** Arctic sea ice area satellite observations from 1979 to present day (2015) obtained from The Cryosphere Today project of the University of Illinois.

[Title Page](#)[Abstract](#)[Introduction](#)[Conclusions](#)[References](#)[Tables](#)[Figures](#)[◀](#)[▶](#)[◀](#)[▶](#)[Back](#)[Close](#)[Full Screen / Esc](#)[Printer-friendly Version](#)[Interactive Discussion](#)

## Early warning signals

M. S. Williamson et al.

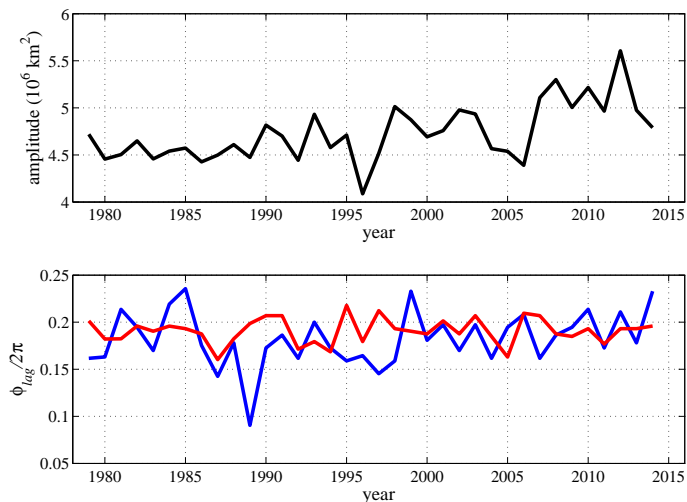


**Figure 7.** In the upper panel amplitude of sea ice area oscillation within each annual is plotted against year and in the lower panel phase lag between the sea ice area minimum (red line) and maximum (blue line) and the solar insolation minimum and maximum are plotted. The oscillation amplitude is increasing however the phase lag is not.

[Title Page](#)[Abstract](#)[Introduction](#)[Conclusions](#)[References](#)[Tables](#)[Figures](#)[Back](#)[Close](#)[Full Screen / Esc](#)[Printer-friendly Version](#)[Interactive Discussion](#)

## Early warning signals

M. S. Williamson et al.

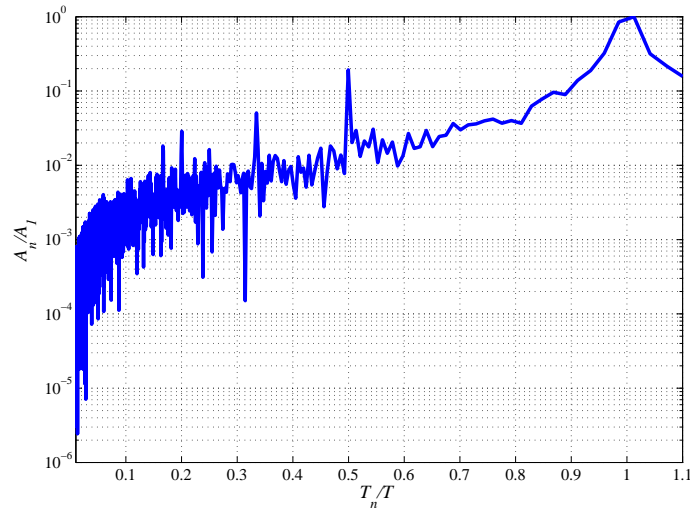


**Figure 8.** Ratio of the  $n$ th order harmonic amplitude to the fundamental harmonic amplitude  $A_n/A_1$  found from the Fourier transform of the Arctic sea ice area time series against the ratio of the  $n$ th harmonic period to the fundamental harmonic period  $T_n/T$ .

[Title Page](#)[Abstract](#)[Introduction](#)[Conclusions](#)[References](#)[Tables](#)[Figures](#)[◀](#)[▶](#)[◀](#)[▶](#)[Back](#)[Close](#)[Full Screen / Esc](#)[Printer-friendly Version](#)[Interactive Discussion](#)